

## Investigation of surface charges, $N_2(A^3\Sigma_u^+)$ metastables and the discharge development in diffuse barrier discharges operating in $N_2$

M. Bogaczyk, S. Nemschokmichal, J. Meichsner, H.-E. Wagner

*Institute of Physics, University of Greifswald, Greifswald, Germany*

### Introduction

Barrier discharges (BDs) have found many applications, e.g. for the ozone synthesis, surface treatment and excimer lamps [1] and still have a high technological potential. The investigation of the elementary processes in the discharge volume as well as the interaction with dielectric surfaces is necessary to get a detailed understanding of the mechanisms (ignition, discharge mode, stability, etc.). For example, the combination of surface charge measurements and the detection of metastables in one (new developed) discharge cell configuration might clarify the importance of the exoemission of electrons from charged surfaces by metastables. The diffuse so-called atmospheric pressure Townsend-like discharge (APTD) in pure nitrogen was investigated.

### Experimental set-up

The set-up of the discharge cell shown in figure 1 consists of two parallel dielectric electrodes at a gap distance of 1 mm. The upper dielectric is a glass plate ( $\epsilon_{\text{glass}} = 7.6$ ) covered with a transparent and conductive ITO layer on its topside. The latter enables the electrical contacting of the external voltage. On top of the grounded and polished aluminium mirror an electro-optic BSO crystal ( $\text{Bi}_{12}\text{SiO}_{20}$ ,  $\epsilon_{\text{BSO}} = 56$ ) allows the surface charge measurement due to its birefringent properties.

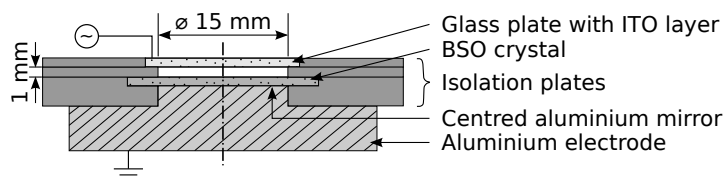


Figure 1: Side-view of the discharge cell configuration.

The application of the optical diagnostics and the gas flow are realized by sidewise orifices. The working gas is pure nitrogen at a pressure from 500 hPa to 1000 hPa. The applied sinusoidal voltage (2 kHz to 5 kHz) amounts up to 6 kV amplitude depending on the gas pressure.

The discharge emission evolution was investigated with the well-established cross-correlation spectroscopy (CCS) diagnostics. In principle, it is based on the time-correlated single photons counting from about  $10^6$  consecutive discharges. Because the BD operates in the diffuse mode, the measurement is triggered electrically [2]. The spatial and spectral resolution are 0.05 mm

and 0.1 nm, respectively. The dominating bands of the second positive system (SPS, 0-0 transition at  $\lambda = 337$  nm) and first negative system (FNS, 0-0 transition at  $\lambda = 391$  nm) have been investigated.

The surface charges are measured temporally and phase resolved under utilization of the electro-optic Pockels effect [3]. For this, the BSO crystal is homogeneously illuminated by a red LED ( $\lambda = 634$  nm). The initially linearly polarized light is changed to elliptic polarization via a  $\lambda/8$  wave plate and the BSO crystal. The ellipticity depends on the voltage drop across the BSO crystal and thus on the BSO surface deposited charges. A linear polarization filter placed in front of a high-speed camera (exposure time 10  $\mu$ s) enables the measurement of the corresponding light intensity changes. The latter allows the recalculation of surface charge densities (sign and value) [4].

The detection of the metastable  $N_2(A^3\Sigma_u^+)$  state is performed by the laser induced fluorescence spectroscopy (LIF). The laser beam (dye: pyridine 1, linewidth:  $0.6\text{ cm}^{-1}$ , pulse energy:  $< 5$  mJ) is focused in front of the discharge cell and has a vertical extend in the discharge centre of about 0.15 to 0.2 mm. It excites the transition from the  $A^3\Sigma_u^+, v = 0$  state to the  $B^3\Pi_g, v = 3$  state at  $\lambda = 687.44$  nm. The following fluorescence from the transition to the  $A^3\Sigma_u^+, v = 1$  state at about 762 nm is measured perpendicularly to the laser beam via a monochromator and a photomultiplier tube. The absolute density calibration is based on the comparison with Rayleigh scattering at carbon dioxide [5, 6].

## Results and discussion

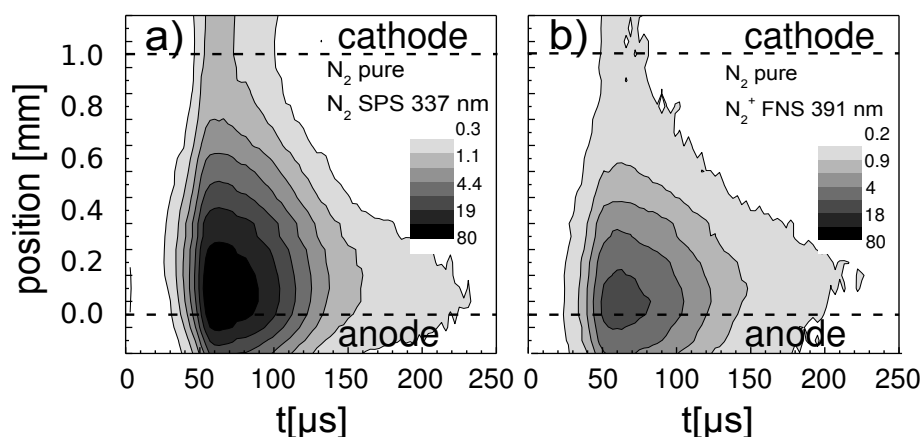


Figure 2: Spatio-temporally resolved discharge developments of the SPS (a) and FNS (b) in pure nitrogen. 500 hPa, 2 kHz, 3.7 kV in pure nitrogen.

As expected, in pure nitrogen the discharge operates in the Townsend-like mode (APTD) [2, 7, 8]. The corresponding spatio-temporally and spectrally resolved optical emission evolu-

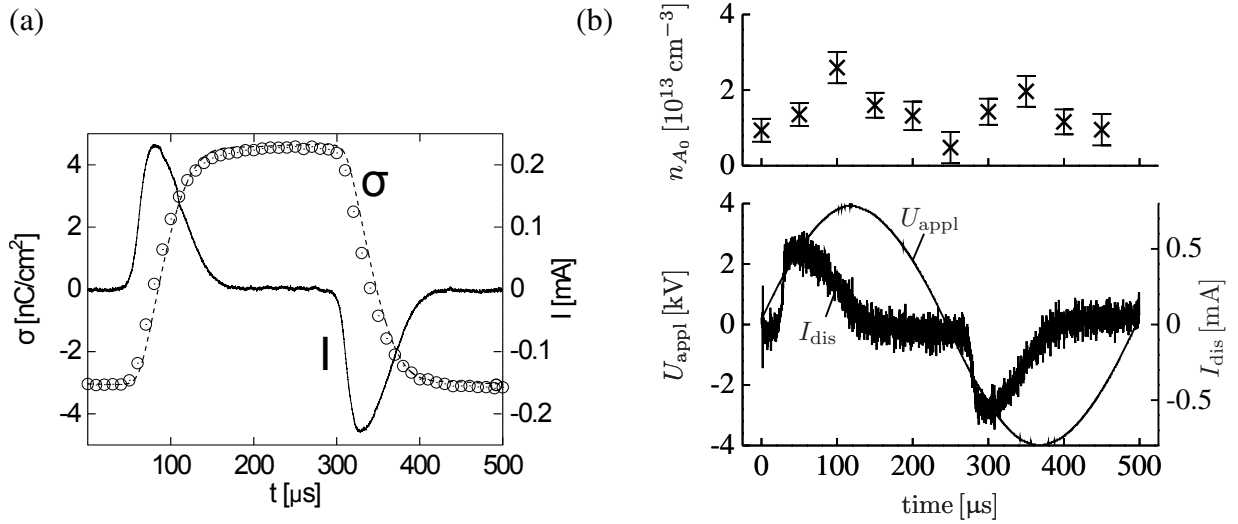


Figure 3: Temporal development of (a) surface charges and (b)  $\text{N}_2(A^3\Sigma_u^+)$  metastables in pure nitrogen (500mbar, 2kHz).

tion is shown in figure 2 for the 0-0 transition of the SPS ( $\lambda = 337$  nm) and the FNS ( $\lambda = 391$  nm) which are most intensive. Typical for the APTD is a emission maximum located near the anode which can be clearly seen in figure 2 [4].

Also, the APTD is characterized by a current duration of several tens of microseconds (100  $\mu$ s) coupled with a low net current density in the order of 0.1 mA/cm<sup>2</sup>. Figure 3a) shows the discharge net current (solid line) and the measured surface charges (circles) over one period. The surface charges stay constantly on the BSO surface until the current pulse appears. During the current pulse, the surface charge changes its sign. It differs in both polarities, namely  $\sigma_+ = 4.5$  nC/cm<sup>2</sup> and for  $\sigma_- = -3$  nC/cm<sup>2</sup>. The reason is the asymmetric discharge cell set-up due to the different dielectric electrode materials BSO and glass, respectively [9]. Qualitatively and quantitatively offers the temporally integrated net current (dashed line in figure 3a)) an excellent agreement of the transferred charge to the surface charge measurement.

The temporal development of the  $\text{N}_2(A^3\Sigma_u^+, \nu = 0)$  density in the center of the discharge gap

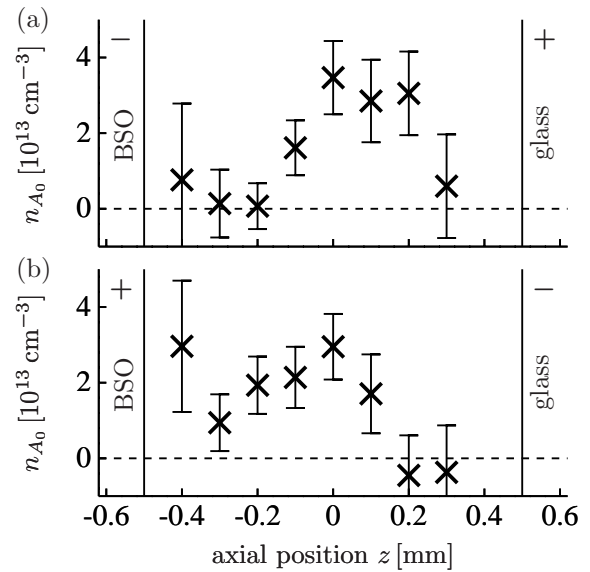


Figure 4: Axial  $\text{N}_2(A^3\Sigma_u^+)$  density profiles in the (a) positive (at 125  $\mu$ s) and (b) negative half cycle (at 375  $\mu$ s).

is shown in figure 3b) in comparison with the applied voltage and the discharge net current. It shows a maximum in each half cycle after the current pulse. The delay of the density maximum with respect to the current pulse is well known from optical-optical double resonance (OODR)-LIF measurements [10] and  $\text{NO}_\gamma$  spectroscopy [10, 11, 12]. The decrease in density after the maximum proceeds within some hundreds of microseconds to a value around  $10^{13} \text{ cm}^{-3}$  at the beginning of the next half cycle.

The spatial distributions of the  $\text{N}_2(A^3\Sigma_u^+, v=0)$  metastables along the central axis are presented in figure 4. Both profiles show a hill shifted to the anode, respectively. This is in agreement with the optical emission in figure 2 and the Townsend-like discharge mode. In contrast, the density of metastables does not increase exponentially towards the anode as the optical emission. In front of the cathode, the density is nearly zero, indicating a fast depletion of metastables in front of the dielectrics. The reason might be quenching of metastables by etching products from the dielectrics as discussed in [13].

### Acknowledgement

Founded by “Deutsche Forschungsgemeinschaft, Sonderforschungsbereich TRR-24, project B11”.

### References

- [1] U. Kogelschatz. *Plasma Chem. Plasma Process.*, 23:1–46, 2003.
- [2] K. V. Kozlov, R. Brandenburg, H.-E. Wagner, A. M. Morozov, and P. Michel. *J. Phys. D: Appl. Phys.*, 38:518, 2005.
- [3] A. Yariv. *Quantum electronics*. WILEY New York, 1989.
- [4] M. Bogaczyk, S. Nemschokmichal, A. Zagoskin, G. B. Sretenović, J. Meichsner, and H.-E. Wagner. *J. Adv. Oxid. Technol.*, 15:310–320, 2012.
- [5] S. Nemschokmichal, F. Bernhardt, B. Krames, and J. Meichsner. *J. Phys. D: Appl. Phys.*, 44:205201, 2011.
- [6] S. Nemschokmichal and J. Meichsner.  $\text{N}_2(A^3\Sigma_u^+)$  metastable density in nitrogen barrier discharges: I. LIF diagnostics and absolute calibration by Rayleigh scattering. submitted to *Plasma Sources Sci. Technol.*
- [7] R. Brandenburg, Z. Navrátil, J. Jánšký, P. Stáhel, D. Trunec, and H.-E. Wagner. *J. Phys. D: Appl. Phys.*, 42:085208, 2009.
- [8] H. Luo, Z. Liang, X. Wang, Z. Guan, and L. Wang. *J. Phys. D: Appl. Phys.*, 43:155201, 2010.
- [9] L. Stollenwerk and U. Stroth. *Contrib. Plasma Phys.*, 51(1):61–67, 2011.
- [10] G. Dilecce, P. F. Ambrico, and S. De Benedictis. *Plasma Sources Sci. Technol.*, 16:511, 2007.
- [11] N. Gherardi, G. Gouda, E. Gat, A. Ricard, and F. Massines. *Plasma Sources Sci. Technol.*, 9:340, 2000.
- [12] R. Brandenburg, V. A. Maiorov, Yu. B. Golubovskii, H.-E. Wagner, J. Behnke, and J. F. Behnke. *J. Phys. D: Appl. Phys.*, 38:2187, 2005.
- [13] N. Gherardi and F. Massines. *IEEE Trans. Plasma Sci.*, 29:536–544, 2001.